Construction and Building Materials 25 (2011) 3941–3949

Contents lists available at ScienceDirect

Construction and Building Materials

journal homepage: www.elsevier.com/locate/conbuildmat

Effect of coarse aggregate size and cement paste volume on concrete behavior under high triaxial compression loading

Xuan Hong Vu [a,*], Laurent Daudeville [b], Yann Malecot [b]

[a] Université de Lyon, Université Lyon 1, Laboratoire Génie Civil et Ingénierie Environnementale (LGCIE), INSA de Lyon, 82 bd Niels Bohr, F-69622 Villeurbanne, France
[b] Université Joseph Fourier – Grenoble 1/INPG/CNRS, 3SR Lab, BP53, 38041 Grenoble cedex, France

ARTICLE INFO

Article history:
Received 14 October 2010
Received in revised form 20 March 2011
Accepted 14 April 2011
Available online 6 May 2011

Keywords:
Concrete
Coarse aggregate size
Coarse aggregate volume
Cement paste volume
Triaxial test
High confinement
High stress

ABSTRACT

When massive concrete structures (high-rise buildings, tunnels, dams, nuclear power plants, bridges, protection structures, ...) are subjected to extreme loadings (aircraft shocks, rock falls, near-field detonations, ballistic impacts, ...), the material undergoes triaxial compression loading at a high confinement. In order to reproduce high stress levels with well-controlled loading paths, static triaxial tests are carried out on concrete samples by mean of a very high-capacity triaxial press. It is a well-known fact that the cement paste volume and the coarse aggregate size are two important parameters of concrete formulation. This article focuses on identifying the effect of coarse aggregate size and cement paste volume on concrete behavior under high triaxial compression. This article shows that at low confinement, the concrete strength slightly increases as the coarse aggregate size increases. At high confinement, the coarse aggregate size has a slight influence on concrete deviatoric behavior and a significant influence on concrete strain limit-state. The higher the coarse aggregate size, the lower is the mean stress level corresponding to concrete strain limit-state. Furthermore, this article highlights that at low confinement, the concrete strength significantly increases with an increase in cement paste volume. Increasing confinement tends to reduce cement paste volume effect on concrete strength. At high confinement, contrary to what has been observed in unconfined compression, the cement paste volume has little effects on concrete deviatoric behavior. Otherwise, decreasing cement paste volume increases concrete deformation capacity. At very high confinement levels and at very high deviatoric stress levels, the axial tangent stiffness of concrete increases as the coarse aggregate size or the cement paste volume is reduced.

1. Introduction

Concrete is employed in the building of highly sensitive infrastructure (high-rise buildings, tunnels, dams, nuclear power plants, bridges, protection structures, ...). Its mechanical behavior however is still rather poorly understood, especially under extreme dynamic loadings (impacts of vehicles or aircrafts, rock falls, near field detonation, ballistic impacts, ...). When subjected to violent dynamic loadings, concrete undergoes very high levels of triaxial stresses [1]. The validation of concrete constitutive models, taking into account simultaneously the brittle damage phenomena and irreversible strain in compaction, requires specific tests capable of reproducing complex loading paths.

The static characterization of a constitutive model to predict the dynamic behavior is not a new practice in the study of geomaterials. The rheological behavior of concrete under confined compression slightly depends on the strain rate for dried or wet specimens [2]. Thus, the strain rate effect in compression can be neglected in numerical simulations [3]. The strong loading rate dependency in tension can mainly be explained by the influence of propagation velocity of defects [4] and must be taken into account in simulations.

Most of the available experimental results in literature only relate to confined concrete behavior with moderate confining pressure [5–11]. These studies have particularly revealed the transition from brittle to ductile behavior that characterizes cohesive materials. Experimental studies on the triaxial behavior of cementitious materials under high confinement were carried out previously but they were limited to small mortar samples [12,13]. Some scarce triaxial test results on ordinary concrete with confining pressures ranging between 0 and 500 MPa are available in [1,14,15].

The results presented in this article make reference to static triaxial tests carried out on concrete samples by mean of a high-capacity hydraulic triaxial press, named the GIGA press. This experimental device makes it possible to reach, within concrete samples, stress levels on the order of one GPa with static, homogeneous and well-controlled load paths.

* Corresponding author. Tel.: +33 4 72 69 20 71; fax: +33 4 78 94 69 06.
E-mail addresses: Xuan-Hong.Vu@univ-lyon1.fr (X.H. Vu), laurent.daudeville@ujf-grenoble.fr (L. Daudeville), yann.malecot@ujf-grenoble.fr (Y. Malecot).

0950-0618/$ - see front matter © 2011 Elsevier Ltd. All rights reserved.
doi:10.1016/j.conbuildmat.2011.04.026

Some previous results on the behavior under high confinement of the same reference ordinary concrete were obtained with the GIGA press. Gabet et al. studied the influence of loading path [16], Poinard et al. highlighted the damage process [17], Dupray et al. developed a mesoscopic model of these experiments [18], Vu et al. studied the influence of both the saturation ratio [19] and the water/cement ratio of concrete [20]. In particular, these results showed that under high confinement, the limit-state of the concrete remains relatively independent of both the loading path and Lode's angle, the saturation ratio exerts a major influence on concrete behavior and, when placed under high confinement, concrete behaves like a granular stacking composed of concrete without any influence from the level of cement matrix strength.

To the best of our knowledge, no results are available regarding the effects of coarse aggregate size and cement paste volume (or coarse aggregate volume) on concrete behavior when subjected to high triaxial compression loading, the present article focuses on these effects.

The experimental set-up used to perform the current study will be described in Section 2. Section 3 will present the main results concerning the effect of coarse aggregate size. Section 4 will introduce the influence of cement paste volume (or the influence of coarse aggregate volume). The presentation of the main conclusions and the outlook of the future work end the paper.

2. Experimental set-up

The GIGA press is a large-capacity triaxial press, which has been specifically designed and developed for this study. Cylindrical concrete specimens ($\varnothing = 70$ mm; h = 140 mm) can be tested by applying confining pressures as large as 0.85 GPa and axial stresses up to 2.35 GPa. A picture of the press and a section of the specimen and of the loading apparatus are shown in Fig. 1 [34,35].

The concrete specimen, surrounded by a membrane impermeable to the confinement fluid, is placed between caps made of tungsten carbide. The instrumentation of the specimens consists of one Linear Variable Differential Transformers (LVDT) for measuring the axial displacement, one axial gauge and two circumferential gauges (Fig. 2).

The LVDT sensor used in this study is 500XS-3013 type from Schaevitz Sensors Company. The gauges (EP-08-10CBE-12 type from Vishay Micro-measurements Company) are 28 mm long. These gauges allow strain measurements up to 15%. Both the axial stress applied to the specimen and the pressure inside the cell are monitored by means of force and pressure sensors. The porous nature of the concrete requires the development of a protective multi-layer membrane surrounding the specimen in order to prevent the confining fluid from infiltrating the specimen [34,35] (see Fig. 2).

Compressive stresses and contraction strains are assumed to be positive; the following symbols are used: σ_x = principal axial stress; p = pressure inside the confining cell; σ_m = mean stress; q = principal-stress difference (deviatoric stress); ε_v = volumetric strain; ε_x = axial strain; and ε_θ = circumferential strain:

$$\sigma_m = \frac{\sigma_x + 2p}{3} \quad q = \sigma_x - p \quad \varepsilon_v = \varepsilon_x + 2\varepsilon_\theta$$

All tests were carried out according to the same triaxial compression loading procedure (Fig. 3). The test begins with a hydrostatic phase, during which confining pressure increases at a rate of 1.67 MPa/s until reaching the desired pressure. The confining pressure is applied on every surfaces of the sample through the membranes or through the two caps until the desired pressure p. Note that for all triaxial tests in this study, the sealing between the loading heads and the top and bottom ends of the concrete specimen is ensured by the multi-layer membrane placed around the specimen and supported over a part of the loading heads. Besides, for triaxial compression loading, there is no sealing between the loading heads and the piston (Fig. 1) [34]. The deviatoric phase is then conducted, at constant confining pressure, by imposing a constant displacement rate of 20 μm/s for the axial jack. This rate corresponds to a strain rate of approximately 10^{-4}/sec for the sample. Note that in all tests the maximum deviatoric stress value is not imposed, as a direct measure of the test. The unloading phase is symmetrical in comparison with the loading phase. Tests were carried out with the control of the confining pressure p and of the piston displacement (Fig. 1).

The unconfined compression tests were performed on a 100 tons Schenck press with a more adequate and accurate load sensor. These tests were controlled in displacement with a strain rate of approximately 10^{-5}/sec. The concrete samples have the same dimensions as those used in the triaxial tests.

3. Influence of coarse aggregate size

In order to study the effect of coarse aggregate size, from the mix design of the reference concrete (R30A7), two other concretes ($d_{\min}$) and ($D_{\max}$) were prepared with different maximum aggregate size (d_a). Compared to concrete R30A7 (d_a = 8 mm), concrete $d_{\min}$ has smaller aggregates (d_a = 3.15 mm), while concrete $D_{\max}$ has larger aggregates (d_a = 20 mm).

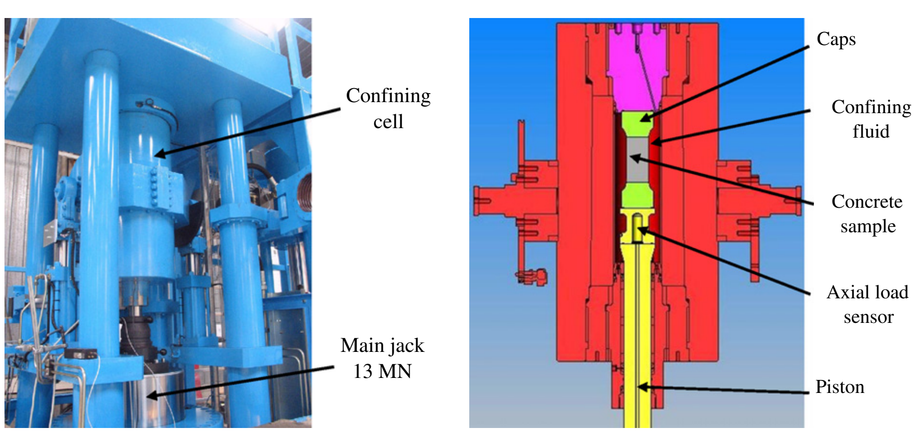

Fig. 1. General view of the GIGA press (left) and cross-section of the confining cell (right).

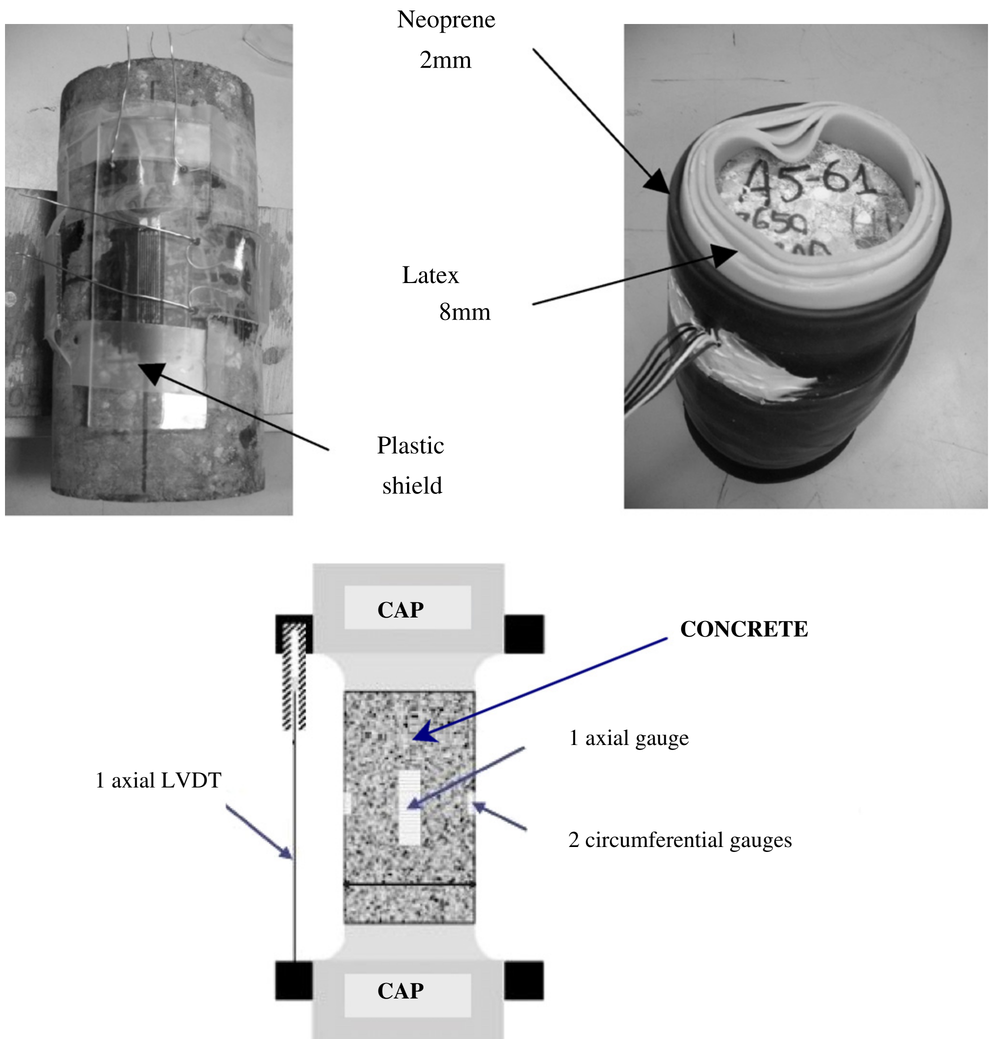

Fig. 2. Instrumentation and protective membrane.

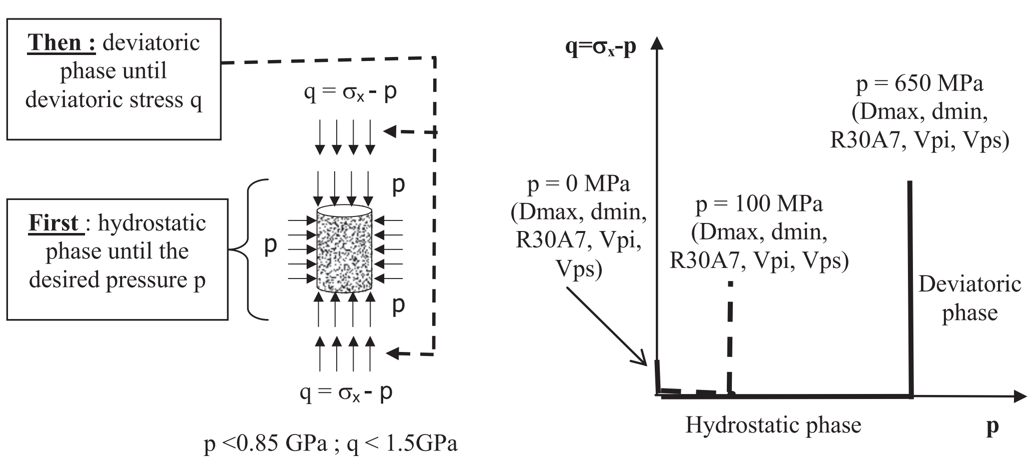

Fig. 3. Loading path of the completed tests: deviatoric stress q vs. confining pressure p; σ_x: axial stress; D_{max}, d_{min}, R30A7, V_{pi}, V_{ps}: five concretes studied in this article.

3.1. Characteristics of concrete samples

3.1.1. Concrete composition

The modified mix designs are shown in Table 1, where the mix design of the reference concrete R30A7 is indicated as well. The composition of the reference concrete, for which an exhaustive experimental study was carried out [16,17,19], is provided in the R30A7 column of Table 1. This reference concrete corresponds to an ordinary concrete in terms of both strength and slump. It displays a 28-days compressive strength of 30 MPa and a slump of

Table 1
Mix design and porosity of concretes d_{min}, D_{max} and R30A7 characterized by different values of the maximum aggregate size (d_a). "D"$^{(*)}$: diameter of aggregates.

Concrete mix design (kg/m^3) and porosity (%)	d_{min}	R30A7	D_{max}
2/3.15 mm "D"$^{(*)}$ gravel (d_a = 3.15 mm)	1006		–
0.5/20 mm "D" gravel (d_a = 20 mm)	–		995
0.5/8 mm "D" gravel (d_a = 8 mm)	–	1008	–
1800 μm "D" sand	838	838	838
CEM I 52.5N PM ES CP2 cement (Vicat)	263	263	263
Water	169	169	169
Porosity accessible to mercury (%)	11.5	12.6	10.7
Cement paste volume (m^3/m^3 of concrete)	0.29	0.29	0.29

7 cm. It can however be noted that the very high quality cement used, for purposes of better controlling material reproducibility, leads to a particularly low cement volume. Aggregates compound 99% quartzite are derived from natural deposit (rolled aggregates). Its maximal size (8 mm) was selected by taking the sample diameter (70 mm) into account.

Both modified mixes (d_{min} and D_{max}) have the same cement paste volume (total volume of water, cement and occluded air measured in fresh concrete) and the same aggregate volume found in the reference mix (R30A7). Gravel 0.5/8 mm "D" is replaced with gravel 2/3.15 mm "D" in mix of d_{min} and with gravel 0.5/20 "D" in mix of D_{max}. Aggregates of concretes d_{min} and D_{max} also compound 99% quartzite are derived from natural deposit (rolled aggregates). The granulometric curves are given in Fig. 4. The porosity (Table 1) was measured by means of a high-pressure mercury-intrusion porosimeter. The values are similar because the three concretes have the same cement paste volume and the same aggregate volume.

The granulometry of concrete R30A7 was established by means of the rather empirical Dreux's method [36], in order to optimize the compactness of the granular skeleton. Hence, any change of coarse aggregate size with respect to the reference concrete leads to a non-optimal compactness of the granular skeleton. In more detail, any reduction of the coarse aggregate size contributes to the reduction of the compactness of the mix and to the increase of the friction between the cement paste and the aggregate particles. Conversely, any increase of coarse aggregate size implies a larger granular range and leads to a better compactness.

3.1.2. Sample making and conservation

A suitable procedure for manufacturing the specimens was established in order to minimize the variability of concrete mechanical properties [34,35]. After cutting the extremities of the specimens to the desired length and smoothing the end sections, all specimens were stored in water for 3 months, in accordance with an identical curing procedure. The specimens were then dried about 4 months in a drying oven at 50 °C and 8% RH. Mass stabilization, however, was reached after 1 month, when the daily variation – after the spell inside the oven – did not exceed 0.1%.

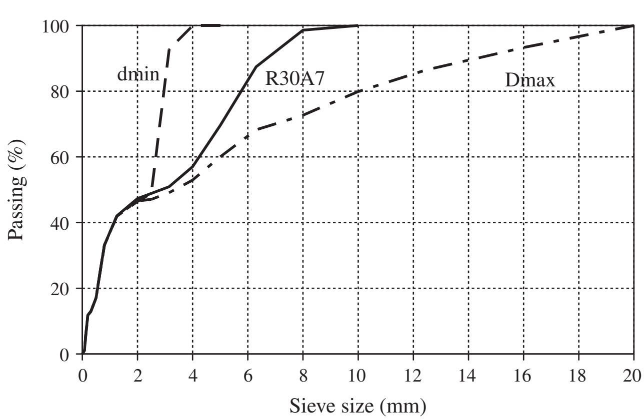

Fig. 4. Granulometric curves of concretes R30A7 (reference), d_{min} and D_{max}.

3.2. Results of the triaxial tests

The behaviors of the three concretes d_{min}, D_{max} and R30A7 during the triaxial tests carried out at no confinement (0 MPa, unconfined compression), at 100 MPa and 650 MPa are presented and discussed in the following. For each concrete, because of the identical procedures for conservation and making of all the tested samples, the mechanical properties of the different samples are thus quasi-equivalent to those of the samples tested in simple compression (Table 2).

3.2.1. Unconfined compression tests

In Figs. 5 and 6, the responses of the three concretes (R30A7, d_{min}, D_{max}) tested in unconfined compression are shown, in terms of mean stress vs. volumetric strain, and axial stress vs. circumferential and axial strains. The numerical values of Young's modulus E, ultimate stress σ_{max} and Poisson's ratio ν obtained for the three concretes (R30A7, d_{min}, D_{max}) are listed in Table 2. The slight differences of the volumetric behaviors (Fig. 5) are related to the small differences in terms of porosity (Table 1). Under unconfined compression, both the strength and the Young's modulus increase with the size of the coarse aggregate (Table 2 and Fig. 6). The strength and Young's modulus of concrete D_{max} are the largest and those of concrete d_{minx} are the smallest. This phenomenon can be explained by the physical entanglement of aggregates that contributes to compressive strength and fracture energy of concrete and that is more pronounced with larger aggregates [25,26]. These results are coherent with those observed in the literature [21–26].

3.2.2. Tests carried out at 100 MPa confinement

In Figs. 7 and 8, the results of the triaxial tests carried out on the three concretes (D_{max}, R30A7, d_{min}) at 100 MPa confinement are shown. Fig. 7 shows that during the initial hydrostatic loading process, the volumetric responses of the three concretes are similar because of their similar porosities (see Table 1). Fig. 8 indicates that the conclusions obtained in the case of unconfined compression are still valid. At 100 MPa confinement level, concrete deviatoric behavior exhibits a stress threshold (peak deviatoric stress or extended plateau). This behavior can be explained by that at 100 MPa confinement, the cement matrix has not been sufficiently damaged during hydrostatic loading. At higher confinement level, when the cement matrix has completely damaged during hydrostatic loading [20], concrete displays a strain-hardening deviatoric behavior (as the case shown in the next paragraph).

3.2.3. Tests carried out at 650 MPa confinement

Figs. 9 and 10 (a close-up of Fig. 9) and 11 show the results of the triaxial tests carried out on the three concretes (D_{max}, R3A7, d_{min}) at 650 MPa confinement. Two tests were carried out on

Table 2
Unconfined compression tests carried out on the three concretes R30A7, d_{min} and D_{max}: identification of the main concrete characteristics.

Concrete	d_{min}	R30A7	D_{max}
Maximum aggregate size (mm)	3.15	8	20
Ultimate stress, σ_{max} (MPa)	41	42	48
Young's modulus, E (GPa)	21.6	24.0	26.7
Poisson's ratio, ν	0.12	0.14	0.18

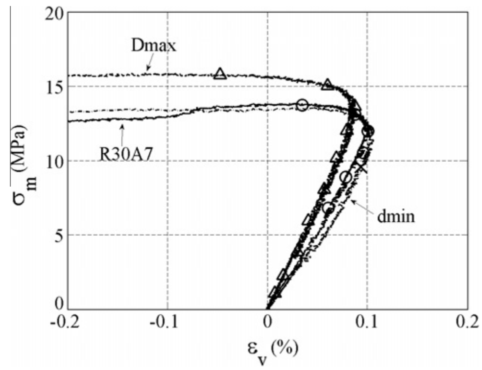

Fig. 5. Unconfined compression: plots of the mean stress σ_m vs. the volumetric strain ε_v for concretes R30A7 (*o*, solid line), $d_{\min}$ (*x*, dash-dot line) and $D_{\max}$ (triangle, dash line).

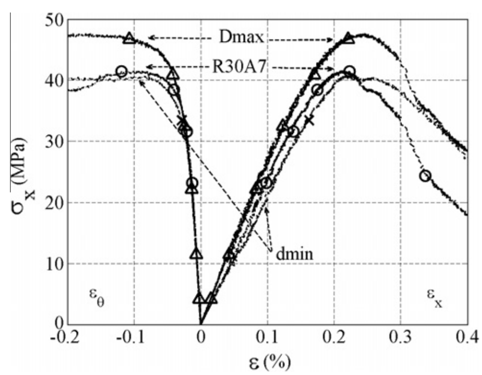

Fig. 6. Unconfined compression: plots of the axial stress σ_x vs. the strains ε_x and ε_θ for concretes R30A7 (*o*, solid line), $d_{\min}$ (*x*, dash-dot line) and $D_{\max}$ (triangle, dash line).

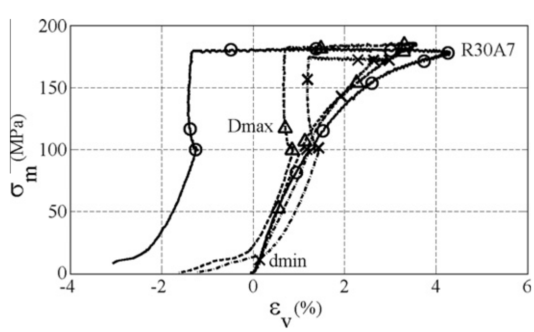

Fig. 7. Triaxial compression at 100 MPa confinement: plots of the mean stress σ_m vs. the volumetric strain ε_v for concretes R30A7 (*o*, solid line), $d_{\min}$ (*x*, dash-dot line) and $D_{\max}$ (triangle, dash line).

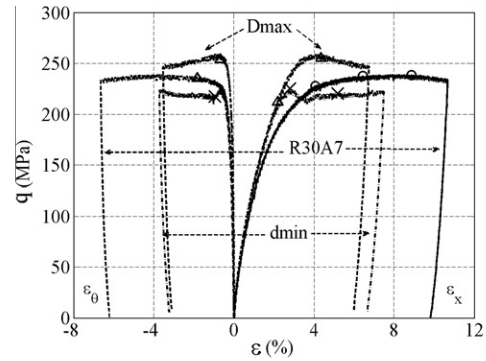

Fig. 8. Triaxial compression at 100 MPa confinement: plots of the stress deviator q vs. the strains ε_x and ε_θ for concretes R30A7 (*o*, solid line), $d_{\min}$ (*x*, dash-dot line) and $D_{\max}$ (triangle, dash line).

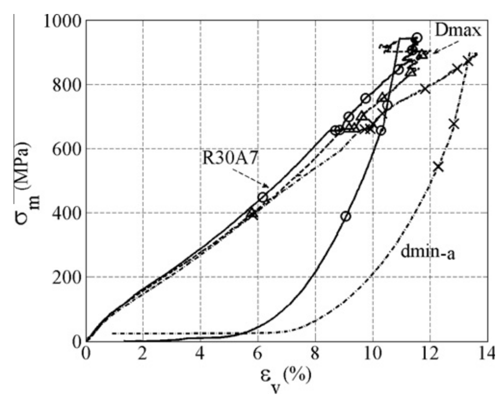

Fig. 9. Triaxial compression at 650 MPa confinement: plots of the mean stress σ_m vs. the volumetric strain ε_v for concretes R30A7 (*o*, solid line), $d_{\text{min-a}}$ (*x*, dash-dot line) and $D_{\max}$ (triangle, dash line).

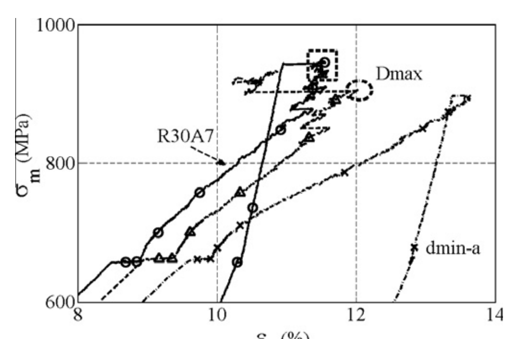

Fig. 10. Close-up of Fig. 9: triaxial compression at 650 MPa confinement: plots of the mean stress σ_m vs. the volumetric strain ε_v for concretes R30A7 (*o*, solid line), $d_{\text{min-a}}$ (*x*, dash-dot line) and $D_{\max}$ (triangle, dash line). Contraction–dilatancy transition: square symbol for concrete R30A7 and ellipse symbol for concrete $D_{\max}$.

concrete $d_{\min}$ ($d_{\text{min-a}}$ and $d_{\text{min-b}}$), but in the former test both the LVDT and the gauges were used, while in the latter test only the LVDT was active. These figures confirm previous findings.

The compaction processes of the three concretes in the hydrostatic phase of the loading are similar because of the similar porosities of the materials (Table 1). In the deviatoric phase, the largest volumetric strain is observed in concrete $d_{\min}$. Furthermore, there is a transition from contraction to dilatancy in concretes $D_{\max}$ and R30A7. This transition can be identified in Fig. 10 (square symbol for concrete R30A7 and ellipse symbol for concrete $D_{\max}$). In this figure, the contraction–dilatancy transition of concrete $D_{\max}$ is (σ_m, q) = (906 MPa, 721 MPa) and that of concrete R30A7 is (σ_m, q) = (934 MPa, 830 MPa). This one corresponds to the maximum volumetric-strain state, in terms of contraction in the material; and can be defined as the strain limit-state of the material. Dilatancy of the dried samples under high confinement is explained by a rearrangement of the granular stacking sequence composing the concrete. The shear stresses generate aggregate movement in the matrix, which initially serves to stimulate compaction. Once the maximum compaction level has been reached, the sample expands [16,17,19]. The mean stress level corresponding to this transition is slightly higher in concrete R30A7, whereas no contraction–dilatancy transition was observed in concrete $d_{\min}$, something that may be explained by observing that in this

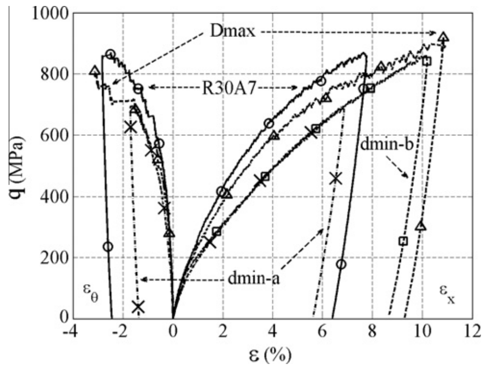

Fig. 11. Triaxial compression at 650 MPa confinement: plots of the stress deviator q vs. the strains ε_x and ε_θ for concrete samples R30A7 (*o*, solid line), $d_{\text{min-a}}$ (*x*, dash-dot line), $d_{\text{min-b}}$ (square, dash line) and D_{max} (triangle, dash line).

concrete the maximum mean stress level (about 950 MPa) does not create the conditions for the contraction–dilatancy transition. Thus, the higher the size of coarse aggregate, the lower is the mean stress level corresponding to the concrete strain limit-state.

The three concretes have a hardening behavior (Fig. 11), as the confining pressure corresponding to the transition between brittle and hardening behaviors has been exceeded (the value of this confining pressure is close to 100 MPa for concrete R30A7 [20], see Fig. 8). Below this confining level, the cement matrix is still cohesive and it is mainly the cement matrix which contributes to concrete response [20]. Above this confining level, the cement matrix has lost its cohesion and it is the stacking of the aggregate particles which governs the concrete response (concrete behaves like a granular material). The ability of the aggregate particles to rotate under shear loading seems to be related to aggregate size. Thus, the higher the aggregate size, the lower is the deformation ability of the concrete.

Contrary to what has been observed in unconfined compression, at 650 MPa confinement, the differences between the plots of the deviatoric stress are rather limited (the maximum difference is about 160 MPa at 6% deviatoric strain). A more thorough examination of the curves in Fig. 11 shows that at high deviatoric strain levels (above 6%) the axial tangent stiffness of concrete d_{min} is higher than that of concrete D_{max}.

4. Influence of the cement paste volume

The influence of the cement paste volume (or of the aggregate volume) with constant water/cement ratio, constant gravel/sand ratio and the same aggregate types is now presented.

4.1. Characteristics of concrete samples

Based on the composition of the reference concrete R30A7, two modified mix designs were adopted (Table 3). In comparison with the composition of the concrete R30A7, the first (V_{pi}) has a cement paste volume (total volume of water, cement, occluded air measured in fresh concrete and possibly water-reducing additive) reduced by 0.04 m^3 (per 1 m^3 of concrete) and the second (V_{ps}) has a cement paste volume increased by 0.04 m^3 (Table 3). A volume reduction of the cement paste with constant water/cement ratio requires the amount of water to be reduced; hence, it is necessary to add a water-reducing additive (Sikafluid) to guarantee a slump of at least 70 mm in concrete V_{pi}. Conversely, the concrete V_{ps} is more liquid and should not be vibrated, in order to avoid aggregate segregation. Casting, curing, machining and drying of the specimens made of concretes V_{pi} and V_{ps} were the same as for concrete R30A7 (see Section 3.1.2). The values of the porosity accessible to mercury are presented in Table 3, where it is shown that the smaller the cement paste volume (or the larger the aggregate volume), the larger the porosity.

Table 3
Mix design and porosity of the three concretes tested to study the effect of cement paste volume. $^{(*)}$"*D*": diameter of aggregates.

Concrete mix design (kg/m^3) and porosity (%)	V_{pi}	R30A7	V_{ps}
0.5/8 mm "*D*"$^{(*)}$ gravel	1064	1008	950
1800 μm "*D*" sand	885	838	791
CEM I 52.5N PM ES CP2 cement (Vicat)	221	263	304
Water (water reducing admixture Sikafluid)	138 (5.31)	169	196
Porosity accessible to mercury (%)	15.2	12.6	11.7
Cement paste volume (m^3/m^3 of concrete)	0.25	0.29	0.33

4.2. Results of the triaxial tests

The behavior of the three concretes V_{pi}, V_{ps} and R30A7 during the triaxial tests carried out at no confinement (0 MPa, unconfined compression) and at 100 MPa and 650 MPa confinement is presented in the following. For each concrete, because of the identical procedures for conservation and making of all the tested samples, the mechanical properties of the different samples are thus quasi-equivalent to those of the samples tested in simple compression (Table 4).

4.2.1. Unconfined compression tests

In Figs. 12 and 13, the responses of the three concretes (V_{pi}, R30A7, V_{ps}) tested in unconfined compression are shown, in terms of mean stress vs. volumetric strain and axial stress vs. circumferential and axial strains. The numerical values of Young's modulus E, ultimate stress σ_{max} and Poisson's ratio ν obtained for the three concretes (V_{pi}, R30A7, V_{ps}) are listed in Table 4. Figs. 12 and 13 show that the volumetric strain decreases slightly, while the strength and the Young's modulus increase significantly following the increase of cement paste volume. The strength of concrete V_{ps} is 2.5 times higher than that of concrete V_{pi} (Fig. 13 and Table 4). In fact, the cohesive force between aggregates surfaces within the concretes V_{ps}, R30A7 and V_{pi} in hardened state depends on the cement paste volume filled in the voids between aggregates. With the same quality of cement paste (constant water/cement ratio), the constant gravel/sand ratio and the same aggregate types, the strength and the Young's modulus differences of the three studied concretes are mainly due to the cohesive force differences between aggregates surfaces of these concretes. Note that in comparison with the composition of the concrete R30A7, the concrete V_{pi} has a cement paste volume reduced by 0.04 m^3 (per 1 m^3 of concrete) and the concrete V_{ps} has a cement paste volume increased by 0.04 m^3 (Table 3). For the concrete V_{pi}, there is a lack of cement paste to fill all the voids between aggregates. Conversely, for the concrete V_{ps}, there is an excess of cement paste to fill all the voids between aggregates. Therefore, the cohesive force between aggregates surfaces within the concrete V_{pi} is the worst and the one within the concrete V_{ps} is the best. This

Table 4
Unconfined compression tests carried out on the three concretes V_{pi}, R30A7, V_{ps}: identification of the main concrete characteristics.

Concrete	V_{pi}	R30A7	V_{ps}
Cement paste volume (m^3/m^3 of concrete)	0.25	0.29	0.33
Ultimate stress, σ_{max} (MPa)	21	42	51
Young's modulus, E (GPa)	15.1	24.0	28.5
Poisson's ratio, ν	0.12	0.14	0.16

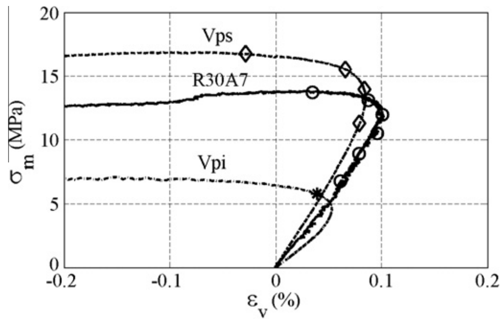

Fig. 12. Unconfined compression: plots of the mean stress σ_m vs. the volumetric strain ε_v for concretes R30A7 (o, solid line), V_{pi} (*, dash-dot line) and V_{ps} (diamond, dash line).

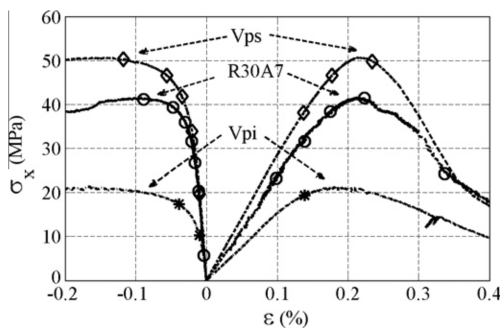

Fig. 13. Unconfined compression: plots of the axial stress σ_x vs. the strains ε_x and ε_θ for concretes R30A7 (o, solid line), V_{pi} (*, dash-dot line) and V_{ps} (diamond, dash line).

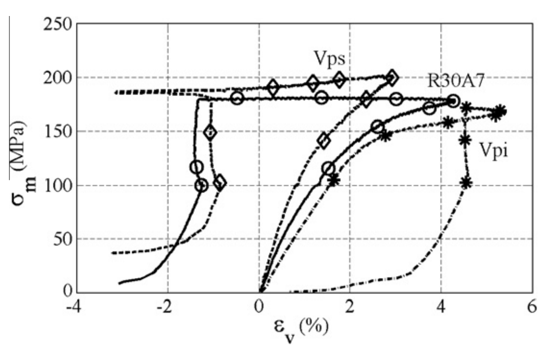

Fig. 14. Triaxial compression at 100 MPa confinement: plots of the mean stress σ_m vs. the volumetric strain ε_v for concretes R30A7 (o, solid line), V_{pi} (*, dash-dot line) and V_{ps} (diamond, dash line).

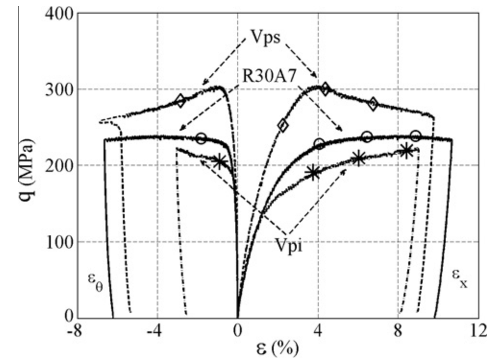

Fig. 15. Triaxial compression at 100 MPa confinement: plots of the stress deviator q vs. the strains ε_x and ε_θ for concretes R30A7 (o, solid line), V_{pi} (*, dash-dot line) and V_{ps} (diamond, dash line).

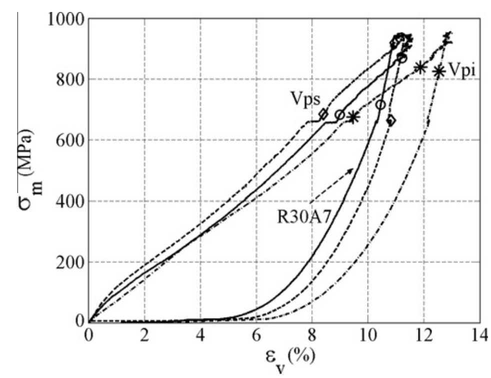

Fig. 16. Triaxial compression at 650 MPa confinement: plots of the mean stress σ_m vs. the volumetric strain ε_v for concretes R30A7 (o, solid line), V_{pi} (*, dash-dot line) and V_{ps} (diamond, dash line).

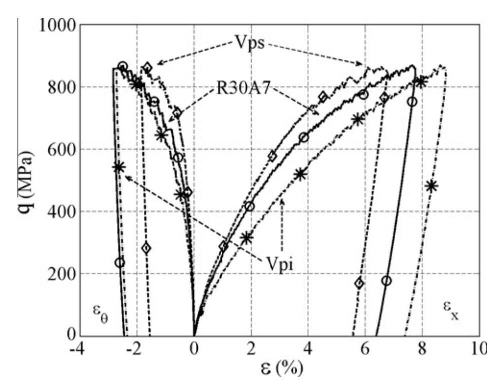

Fig. 17. Triaxial compression at 650 MPa confinement: plots of the stress deviator q vs. the strains ε_x and ε_θ for concretes R30A7 (o, solid line), V_{pi} (*, dash-dot line) and V_{ps} (diamond, dash line).

explains the fact that the strength and the Young's modulus of concrete increase significantly as the cement paste volume increases (Table 4). Furthermore, as could be expected, an increase in the Poisson's ratio of the concrete can be observed with a increase of the cement paste volume (Table 4) because the concrete V_{pi} is the most porous and the concrete V_{ps} is the less porous (Table 3). These results are in agreement with the information available in the literature [27–33].

4.2.2. Tests carried out at 100 MPa confinement

Fig. 14 shows volumetric responses of the three concretes. In this figure, during the initial hydrostatic loading process, the volumetric strain of concrete V_{pi} is highest and that of concrete V_{ps} is lowest. This result is coherent with porosity differences of these concretes (Table 3).

Fig. 15 presents deviatoric responses of the three concretes. One can observe a decrease, compared to the simple compression, of the difference between strengths of the three concretes. Furthermore, concrete V_{ps} has a stress peak, followed by strain softening. Concrete R30A7 shows a ductile behavior with a horizontal plateau. Concrete V_{pi} indicates a strain-hardening behavior.

4.2.3. Tests carried out at 650 MPa confinement

Figs. 16 and 17 show the results of the triaxial tests carried out on the three concretes (V_{ps}, R3A7, V_{pi}) at 650 MPa confinement. At very high confinement levels, a decrease of cement paste volume increases the deformation capacity (Fig. 16), because the phenomena observed at low confinement levels are reversed, as the cementitious matrix is no more cohesive. Fig. 17 indicates that at 650 MPa confinement, the differences between the deviatoric stress of the three concretes are rather limited (the maximum difference is about 200 MPa at 4% axial deviatoric strain). A more thorough observation of the curves in Fig. 17 highlights that for high deviatoric strain levels (above 6%), the larger the cement paste volume, the smaller the axial tangent stiffness of the concrete. Thus, at high confinement levels, any reduction of the cement paste volume increases the deformation capacity of the material; as a result, the deviatoric stress slightly depends on cement paste volume. At high deviatoric strain levels, the larger the cement paste volume, the smaller the axial tangent stiffness.

5. Conclusion and future work

This experimental investigation concerned the effect of coarse aggregate size and cement paste volume on concrete behavior under high triaxial compression loading. To identify this effect, a reference concrete was modified by varying only very few parameters. Triaxial tests were carried out on concrete samples for different coarse aggregate sizes (varying from 3 mm to 20 mm) or for different cement paste volumes (varying from 0.25 m^3 to 0.33 $m^3/1m^3$ of concrete) and for confining pressure levels between 0 MPa and 650 MPa.

The coarse aggregate size has a slight influence on concrete deviatoric behavior as confinement levels vary from 0 MPa to 650 MPa. The concrete strength slightly increases as the coarse aggregate size increases as observed under unconfined compression. The coarse aggregate size has a significant influence on concrete strain limit-state at high confinement, the higher the coarse aggregate size, the lower is the mean stress level corresponding to concrete strain limit-state. At very high confinement levels and at very high deviatoric stress levels, the concrete axial tangent stiffness increases as the coarse aggregate size is reduced.

The cement paste volume has a significant effect on concrete behavior at low confinement. The concrete strength significantly increases with an increase in cement paste volume. Increasing confinement levels tends to reduce cement paste volume effect on concrete strength. At high confinement levels, contrary to what has been observed in unconfined compression, the cement paste volume has little effects on concrete deviatoric behavior. Otherwise, decreasing cement paste volume increases concrete deformation capacity. At very high confinement levels and at very high deviatoric stress levels, decreasing cement paste volume increases concrete axial tangent stiffness.

From an application standpoint, the presented results show that the strength of concrete, when subjected to extreme dynamic loading, is slightly influenced by the coarse aggregate size or by the cement paste volume for mean stress levels below 950 MPa and deviatoric stress levels below 900 MPa. This observation is contrary to the one issued from compression tests performed under moderate confinement, including unconfined compressive tests, in which the concrete compressive strength essentially depends on the cement paste quality and quantity and slightly depends on the coarse aggregate size. In reality, the cement is usually one of the most expensive constituents of concrete. The results shown in this article highlight the mechanical and economic advantages derived by reducing the cement paste volume (or the cement content) of concrete structures subjected to extreme loadings. Otherwise, many of the available protective design guidelines recommend the use of empirical approaches for the assessment of penetration, scabbing and perforation of concrete structures submitted to impacts [37]. All these empirical approaches consider the unconfined compressive strength as the only material parameter governing the resistance of concrete structures. The results presented in this article show the need to complement these empirical approaches to better take into account the influence of the granular skeleton of concrete into its resistance to impact.

As for the test set-up used in this study, axial stresses as large as 1.6 GPa can be applied to concrete specimens (diameter 70 mm; length 140 mm). However, the set-up will be partly modified in order to accommodate smaller specimens (diameter 50 mm; length 105 mm) in order to induce higher deviatoric stresses. In this way, the roles played by coarse aggregate size and cement paste volume will be more thoroughly investigated with reference to concrete deviatoric behavior.

Acknowledgments

This research project was financially supported by the "Centre d'Etudes de Gramat" (CEG, DGA, French Ministry of Defense). We would like to thank Dr. Eric Buzaud and Dr. Christophe PONTIROLI (CEA-Gramat) for giving technical and scientific advice.

References

[1] Warren T, Fossum A, Frew D. Experimental investigation of size effect in concrete fracture under multiaxial compression into low-strength (23 MPa) concrete: target characterization and simulations. Int J Impact Eng 2004;30: 477–503.
[2] Forquin P, Safa K, Gary G. Influence of free water on the quasi-static and dynamic strength of concrete in confined compression tests. Cem Concr Res 2010;40(2):321–33.
[3] Hentz S, Donze F, Daudeville L. Discrete element modelling of concrete submitted to dynamic loading at high strain rates. Comput Struct 2004;82(29–30):2509–24.
[4] Hild F, Denoual C, Forquin P, Brajer X. On the probabilisticdeterministic transition involved in a fragmentation process of brittle materials strains. Comput Struct 2003;81(12):1241–54.
[5] Li H, Pugh D. Mechanical behaviour of materials under pressure. Elsevier; 1970.
[6] Kupfer HB, Gerstle KH. Behavior of concrete under biaxial stresses. J Eng Mech Div 1973;99(4):853–66.
[7] Imran I, Pantazopoulou SJ. Experimental study of plain concrete under triaxial stress. ACI Mater J 1996;93(6):589–601.
[8] Sfer D, Carol I, Gettu R, Etse G. Study of the behavior of concrete under triaxial compression. J Eng Mech ASCE 2002;128(2):156–63.
[9] Berthet JF, Ferrier E, Hamelin P. Compressive behavior of concrete externally confined by composite jackets. Part A: experimental study. Constr Build Mater 2004;19(3):223–32.
[10] Petkovski M, Crouch RS, Waldron P. Apparatus for testing concrete under multiaxial compression at elevated temperature (mac^{2T}). Exp Mech 2006;46: 387–398.
[11] Van Mier JGM. Some notes on microcracking, softening, localization, and size effects. Int J Damage Mech 2009;18:283–309.
[12] Bazant Z, Bishop F, Chang T. Confined compression tests of cement paste and concrete up to 300 ksi. ACI J 1986;33:553–60.
[13] Burlion N, Pijaudier-Cabot G, Dahan N. Experimental analysis of compaction of concrete and mortar. Int J Numer Anal Methods Geomech 2001;25:1467–86.
[14] Akers SA, Phillips BR. Concrete modelled as un inhomogeneous material: numerical simulations of contact detonation charges. In: 18th International symposium on the military aspects of blast and shock, Oberjettenberg, Germany; 2004.
[15] Schmidt JM, Cazacu O, Green ML. Experimental and theoretical investigation of the high-pressure behavior of concrete. Int J Numer Anal Methods Geomech 2009;33:1–23.
[16] Gabet T, Malécot Y, Daudeville L. Triaxial behavior of concrete under high stresses: influence of the loading path on compaction and limit states. Cem Concr Res 2008;38(3):403–12.
[17] Poinard C, Malecot Y, Daudeville L. Damage of concrete in a very high stress state: experimental investigation. Mater Struct 2010;43(1–2):15–29.
[18] Dupray F, Malecot Y, Daudeville L, Buzaud E. A mesoscopic model for the behavior of concrete under high confinement. Int J Numer Anal Methods Geomech 2009;33:1407–23.
[19] Vu XH, Malecot Y, Daudeville L, Buzaud E. Experimental analysis of concrete behavior under high confinement: effect of the saturation ratio. Int J Solids Struct 2009;46:1105–20.
[20] Vu XH, Malecot Y, Daudeville L, Buzaud E. Effect of the water/cement ratio on concrete behavior under extreme loading. Int J Numer Anal Methods Geomech 2009;33(17):1867–88.

[21] Meddah M, Zitouni SS, Belaabes S. Effect of content and particle size distribution of coarse aggregate on the compressive strength of concrete. Constr Build Mater 2010;24:505–12.
[22] Tumidajski PJ, Gong B. Effect of coarse aggregate size on strength and workability of concrete. Can J Civ Eng 2006;33:206–13.
[23] Akçaoglu T, Tokyay M, Celik T. Effect of coarse aggregate size and matrix quality on ITZ and failure behavior of concrete under uniaxial compression. Cement Concr Compos 2004;26:633–8.
[24] De Larrard F, Belloc A. The influence of aggregate on the compressive strength of normal and high-strength concrete. ACI Mater J 1997;94(5):417–26.
[25] Kaplan MF. Flexural and compressive strength of concrete as affected by properties of coarse aggregates. ACI J Proc 1959;55(11):1193–208.
[26] Neville AM. Properties of concrete. 4th ed. Pearson Prentice Hall; 2002.
[27] Roziere E, Granger S, Turcry P, Loukili A. Influence of paste volume on shrinkage cracking and fracture properties of self-compacting concrete. Cement Concr Compos 2007;29:626–36.
[28] El-Ariss B. Effect of reducing coarse aggregates on concrete strength. Constr Build Mater 2006;20:149–57.
[29] Amparano FE, Xi Y, Roh YS. Experimental study on the effect of aggregate content on fracture behavior of concrete. Eng Fract Mech 2000;67:65–84.
[30] Stock AF, Hannantt DJ, Williams RIT. The effect of aggregate concentration upon the strength and modulus of elasticity of concrete. Magazine Concr Res 1979;31:225–34.
[31] Singh BG. Specific surface of aggregates related to compressive and flexural strength of concrete. ACI J Proc 1958;54(4):897–907.
[32] Chen B, Liu J. Investigation of effects of aggregate size on the fracture behavior of high performance concrete by acoustic emission. Constr Build Mater 2006;21(8):1696–701.
[33] Chen B, Liu J. Effect of aggregate on the fracture behavior of high strength concrete. Constr Build Mater 2004;18:585–90.
[34] Vu XH, Malecot Y, Daudeville L. Strain measurements on porous concrete samples for triaxial compression and extension tests under very high confinement. J Strain Anal Eng Des 2009;44(8):633–57.
[35] Vu XH. Caractérisation expérimentale du béton sous fort confinement: influences du degré de saturation et du rapport eau/ciment. Editions Universitaires Européennes; 2010; ISBN-13: 9786131504570 or ISBN: 6131504571 [in French].
[36] Dreux G. Nouveau guide du béton. Eyrolles; 1985 [in French].
[37] Li QM, Reid SR, Wen HM, Telford AR. Local impact effects of hard missiles on concrete targets. Int J Impact Eng 2006;32(1–4):224–84.